Biogas upgrading with hydrogenotrophic methanogenic biofilms

Maegaard, Karen; Garcia-Robledo, Emilio; Kofoed, Michael V.W.; Agneessens, Laura M.; de Jonge, Nadieh; Nielsen, Jeppe L.; Ottosen, Lars D.M.; Nielsen, Lars Peter; Revsbech, Niels Peter

Published in:
Bioresource Technology

DOI (link to publication from Publisher):
10.1016/j.biortech.2019.121422

Publication date:
2019

Document Version
Accepted author manuscript, peer reviewed version

Biogas upgrading with hydrogenotrophic methanogenic biofilms

Karen Maegaard, Emilio Garcia-Robledo, Michael V.W. Kofoed, Laura M. Agneessens, Nadieh de Jonge, Jeppe Lund Nielsen, Lars D.M. Ottosen, Lars Peter Nielsen, Niels Peter Revsbech

PII: S0960-8524(19)30652-2
DOI: https://doi.org/10.1016/j.biortech.2019.121422
Article Number: 121422
Reference: BITE 121422

To appear in: *Bioresource Technology*

Received Date: 5 March 2019
Revised Date: 2 May 2019
Accepted Date: 3 May 2019

Please cite this article as: Maegaard, K., Garcia-Robledo, E., Kofoed, M.V.W., Agneessens, L.M., de Jonge, N., Lund Nielsen, J., Ottosen, L.D.M., Peter Nielsen, L., Peter Revsbech, N., Biogas upgrading with hydrogenotrophic methanogenic biofilms, *Bioresource Technology* (2019), doi: https://doi.org/10.1016/j.biortech.2019.121422

Biogas upgrading with hydrogenotrophic methanogenic biofilms

Karen Maegaard[1], Emilio Garcia-Robledo[1,3], Michael V. W. Kofoed[2], Laura M. Agneessens[2], Nadieh de Jonge[4], Jeppe Lund Nielsen[4], Lars D. M. Ottosen[2], Lars Peter Nielsen[1] and Niels Peter Revsbech[1*]

[1] WATEC, Section of Microbiology, Department of Bioscience, Aarhus University, Aarhus, Denmark

[2] Biological and chemical engineering, Department of Engineering, Aarhus University, Aarhus, Denmark

[3]Department of Biology, University of Cadiz, Cadiz, Spain

[4]Department of Chemistry and Bioscience, Aalborg University, Aalborg, Denmark

[*]Corresponding author

16 Abstract

17 Hydrogen produced from periodic excess of electrical energy may be added to biogas reactors
18 where it is converted to CH_4 that can be utilized in the existing energy grid. The major challenge
19 with this technology is gas-to-liquid mass transfer limitation. The microbial conversions in reactors
20 designed for hydrogenotrophic methanogenesis were studied with microsensors for H_2, pH, and
21 CO_2. The H_2 consumption potential was dependent on the CO_2 concentration, but could partially
22 recover after CO_2 depletion. Reactors with 3-dimensional biofilm carrier material and a large gas
23 headspace allowed for a methanogenic biofilm in direct contact with the gas phase. A high density
24 of *Methanoculleus sp*. in the biofilm mediated a high rate of CH_4 production, and it was calculated
25 that a reactor filled with 75% carrier material could mediate a biogas upgrading from 50 to 95%
26 CH_4 within 24 h when an equivalent amount of H_2 was added.

27 Keywords: microsensor, biofilm, CO_2 limitation, methane, methanogenesis, mass transfer

28

29

1. Introduction

The rising concern for the increase in atmospheric CO_2 content and the dependence on fossil fuels emphasize the need for a shift towards renewable energy sources. Renewable energy technologies as wind power and solar power periodically produce energy that cannot be utilized in the power grid. A storage of this excess energy remains one of the major challenges in a society relying on renewable energy sources (Götz et al. 2016).

An important source of renewable energy is biogas produced in anaerobic digesters (Weiland 2010). Sludge, waste, manure, agricultural residues etc. are degraded in anaerobic digesters to produce CH_4 that can be used for electricity and heat production. The organic matter is broken down in a series of reactions yielding a biogas consisting of CH_4 (50-70%), CO_2 (30-50%) and trace gasses. If biogas should be used in the natural gas grid, a CH_4 content of at least 95% and removal of sulfur- and silicon-containing gasses are required. The CO_2 can be removed by various techniques as water scrubbing, scrubbing with organic solvents, pressure swing absorption, chemical washing and membrane technologies (Weiland 2010; Ghorbanian et al. 2014; Gaj 2017; Angelidaki et al. 2018). Another way of removing the CO_2 is to use the excess energy from wind and solar power to produce H_2 that is converted to CH_4 when combining with CO_2 in an anaerobic bioreactor. The upgraded CH_4 can be stored and later utilized on demand (Angelidaki et al. 2018), or it can be converted to more storage friendly fuels as methanol and dimethyl ether (Alvarez-Galvan et al. 2011). Homoacetogenic bacteria also utilize the substrates H_2 and CO_2, producing acetate that subsequently fuel acetotrophic methanogenesis (Angelidaki et al. 2011). Methane has the advantage over H_2 that the volumetric energy density is higher and the infrastructure for CH_4 utilization and storage already exists (Luo et al. 2012).

Hydrogen addition has been successfully applied in small scale reactors where the H_2 was readily consumed by the inherent microbial community (e.g. Luo et al. 2012; Wang et al. 2013; Díaz et al.

2015; Agneesens et al. 2017) and the biogas was upgraded to 95-99% CH_4 (Luo et al. 2012; Wang et al. 2013; Díaz et al. 2015). The reported problems revolve around pH increase and CO_2 limitation (Luo et al. 2012; Bassani et al. 2015; Garcia-Robledo et al. 2016). During anaerobic digestion CH_4 production occurs at pH values of 6.5-8.5 with a pH optimum between 7 and 8, which would make pH control necessary to maintain the CH_4 production in liquid-based reactors for biogas upgrading (Demirel and Scherer 2008; Weiland 2010). The addition of H_2 could cause volatile fatty acids (VFAs) to accumulate in the reactor by inhibiting degradation of VFAs due to the increase in H_2 concentration and due to stimulation of homoacetogenesis leading to acidification and reactor failure (Schmidt and Ahring 1993; Cord-Ruwisch et al. 1997; Liu et al. 2016).

One of the major challenges with the H_2 to CH_4 technology is the introduction of H_2 into the anaerobic digester, where the mass transfer tends to be inefficient due to a low H_2 solubility. Efficient H_2 to liquid mass transfer is essential for developing this technology, ensuring that H_2 is consumed in the reactor and does not escape to the gas phase (Luo et al. 2012). The H_2 can either be introduced *in-situ* to the main reactor or *ex-situ* to a secondary reactor with a specialized design (Angelidaki et al. 2018; Jensen et al. 2018). In small-scale reactors, the H_2 has been introduced by bubbling (Luo et al. 2012; Luo and Angelidaki 2013a; Bassani et al. 2016), hollow fiber membranes (Luo and Angelidaki 2013b; Wang et al. 2013; Díaz et al. 2015), silicone membranes (Garcia-Robledo et al. 2016) and headspace injection (Agneessens et al. 2017). The H_2 injection method needs to be designed so that the gas-liquid contact and gas retention time is extended while the bubble size is decreased (Bassani et al. 2016; Jensen et al. 2018). Hydrogen injection combined with gas recirculation has been tested in a full-scale reactor, but a relatively large bubble size limited full conversion of the H_2 (Jensen et al. 2018). Hollow fiber membranes and silicone tubing/membranes have been shown to facilitate a full conversion of the H_2 without bubbling (Wang et al. 2013; Díaz et al. 2015; Garcia-Robledo et al. 2016), but upscaling of such technologies

may be difficult. A trickling filter supporting a methanogenic biofilm has been implemented in biogas upgrading with H_2, demonstrating that a quite efficient gas-biofilm mass transfer can be obtained with this technology (Rachbauer et al. 2016). Several biofilm carrier materials have been implemented in wastewater treatment and anaerobic digestion to increase the surface area and retain the microbial community (E.g. Pérez et al. 1997; Cresson et al. 2008; Pandey and Sarkar 2007; Gagliano et al. 2017), and there are thus several options to choose among for biogas upgrading based on biofilm technology.

In this study, we seek to address some of the major challenges with biofilm mediated H_2 to CH_4 conversion, focusing on CO_2 limitation and gas-to-liquid mass transfer. The effect of CO_2 depletion was investigated at a microscale by supplying H_2 through a silicone membrane. We hypothesized that supply through a silicone membrane would facilitate full H_2 conversion making it an ideal system to study H_2 conversion and CO_2 limitation by determining the microscale dynamics of H_2, CO_2 and pH under varying CO_2 supply rates. We propose that large headspace reactors, fitted with carrier material covered by methanogenic biofilm, could lower the mass transfer limitations seen by other reactor approaches and thereby promote conversion of H_2 and CO_2 to CH_4. Our hypothesis was tested by measuring microscale H_2 profiles in the biofilms, determining the CH_4 production rates, VFAs accumulation over time, and analyzing the microbial community composition.

2. Materials and methods

2.1 CO_2 limitation of methanogenesis

A mini-reactor with two compartments separated by a silicone membrane was designed according to Garcia-Robledo et al. (2016). The mini-reactor was constructed of a Plexiglas cylinder closed with a rubber stopper in the bottom. The Plexiglas cylinder was separated into two compartments by

a stainless steel mesh (mesh size 0.1 cm) casted into a 0.1 cm thick silicone rubber membrane (Dow Corning 732 Multi-Purpose Sealant). Gas flow through the bottom compartment was ensured by inserting two hypodermic needles through the butyl rubber stopper in the bottom compartment. One needle was connected to a gas mixer (Brooks Instruments 0260 with Thermal Mass Flow Controllers GF40) and the other needle allowed the gas to exit. The gas flow (100 mL · min^{-1}) was conducted through Tygon tubing and all gases were humidified by bubbling through demineralized water to avoid excessive evaporation from the analyzed samples. In the upper compartment, an about 0.5 cm thick layer of digestate mixed with 40-60 µm glass beads rested directly on the silicone membrane. It was necessary to ensure that there was no turbulent mixing in the analyzed digester content during the microsensor analysis, and stabilization with chemically inert glass beads was used to ensure that diffusion was the only means of transport. The upper compartment was covered with Parafilm and flushed with humidified argon. This allowed microsensors to be introduced through a hole in the Parafilm to measure chemical parameters down through the digestate. Samples of mesophilic digester content were obtained from Bånlev biogas plant (Trige, Denmark), sieved through a 0.1 cm mesh and mixed with glass beads for physical stabilization. The digester content was transferred to the experimental set-up within 3 h of sampling. Bånlev biogas plant has a mesophilic reactor treating agricultural waste products with a hydraulic retention time of ~23 days. The CH_4 production rate is 0.6-1 $L_{CH_4} \cdot {L_{slurry}}^{-1} \cdot day^{-1}$. The dynamics and time course of H_2 consumption as affected by CO_2 depletion was investigated by flushing a mixture of 75% H_2 and 25% N_2 through the lower compartment of the mini-reactor. Measurements of H_2, CO_2 and pH were done every second hour until stable profiles were observed. Hereafter, the H_2 was kept at 75% while the CO_2 concentration was gradually increased from 0% and up to 20% to evaluate the relationship between CO_2 concentration and H_2 consumption.

2.2 Methanogenic biofilm

The methanogenic biofilm growing on the carrier material was contained in 1 L serum bottles sealed with a butyl rubber stopper that were regularly flushed with 80% H_2 and 20% CO_2 and incubated at 38 °C. The serum bottles had three 1 cm drilled holes in the side allowing for microsensor profiling of the biofilm. Butyl rubber stoppers sealed the holes except for during profiling. The carrier material tested was EXPO-NET BIO-BLOK Filter Media (EXPO-NET, Denmark A/S). The controls were flushed with either 80% N_2/ 20% CO_2 or 80% H_2/ 20% CO_2 and had no biofilm carrier material. Each treatment had four replicates. All bottles were inoculated with 300 ml digester content from Bånlev Biogas plant leaving a headspace of ~75%. The digester content was sieved through a 0.1 cm screen before inoculation. The liquid phase in the bottles was partially exchanged once a week during the first 5 weeks by removing 10-50 mL and resupplying with mineral medium (Angelidaki et al. 2009). The amount of medium exchange was increased from 10 mL to 50 mL at week 5 since a decrease in the CH_4 production rate was observed. The buffer capacity of the mineral medium had been increased as compared to the original recipe by adding $NaHCO_3$ to a concentration of 0.25 mol $\cdot$ L^{-1} to match the bicarbonate concentration in digestate. The original medium contained Na_2S and resazurin, but these were excluded in the applied medium. To minimize the amount of CH_4 originating from degradation of organic matter, nutrients were only supplied by mineral medium. The bottles were flushed 1-2 times per week with a gas mixture of 80% H_2 and 20% CO_2. The pressure was recorded with a pressure gauge (Keller, Eco 1) before flushing the bottles and adjusted to a slight overpressure of 0.25 bar after flushing. Periodic wetting of the biofilm was achieved by turning the bottles upside down 1-5 times a week. The CH_4 production rates were determined after one, two, five, six, seven and eight weeks of incubation. All the bottles were flushed with a gas mixture of 80% H_2 and 20% CO_2. Gas samples were collected from the headspace with a glass syringe (SGE Analytical Science) by penetrating the

149 butyl rubber stopper with a 0.4 mm hypodermic needle. The gas samples were transferred to Labco
150 Exetainers flushed with N_2. The CH_4 content in the gas samples was determined within 1 day of
151 sampling using a gas chromatograph equipped with a flame ionization detector (SRI Instruments,
152 SRI 310C). Concentration profiles of H_2 were determined in the slurry from the H_2/CO_2 controls
153 and in the biofilms on the BIO-BLOK. The headspace of the bottles was flushed with a humidified
154 mixture of 80% H_2 and 20% CO_2 at 600 mL · min^{-1} during profiling to ensure a defined gas
155 composition and to avoid contamination with air. In the bottles containing the biofilm and carrier
156 material, the microsensor was introduced through the prepared holes while the bottle was oriented
157 horizontally. When H_2 concentration profiles were recorded in the slurry, the microsensor was
158 introduced from above through the neck of the bottle while the diameter of the opening was
159 restricted to ~0.9 cm with Parafilm. Replicate profiles were recorded in several spots. The VFA
160 content of the slurry was analyzed using a gas chromatograph (System 7890A Agilent
161 Technologies, United States), equipped with a flame ionization detector and a HP-INNOWAY
162 column (30 m · 0.250 mm · 0.25 µm) (Agilent Technologies).

163

164 2.3 Sensors and recording of profiles

165 A H_2 microsensor with a sulfide trap making it insensitive to sulfide was applied (Nielsen et al.
166 2015). The H_2 microsensors applied had a tip size of 20-60 µm and a sensitivity of 1.3-6.1 pA ·
167 $(\mu mol \cdot L^{-1})^{-1}$. A newly developed electrochemical CO_2 microsensor (Revsbech et al. 2019) was
168 applied. The CO_2 microsensors had a tip size of 30-60 µm and a sensitivity of 0.03-1.4 pA · (µmol ·
169 $L^{-1})^{-1}$. The least sensitive sensors were made especially for measurement of very high CO_2
170 concentrations as the very sensitive sensors exhibited non-linear response at high CO_2. Since the
171 CO_2 sensor is sensitive to H_2S, the H_2S was removed by adding $FeCl_2$ to a concentration of 5 mmol

172 · L^{-1} before application of the CO_2 microsensor. The absence of H_2S was confirmed by analysis with
173 a H_2S microsensor (Jeroschewski et al. 1996). Microprofiles of CO_2 through pasteurized digester
174 content placed in a similar set-up did not indicate that other substances in the digester content
175 interfered with the CO_2 measurements (data not shown). Further, simultaneous pH profiles were
176 recorded with a pH microelectrode with an external Ag/AgCl reference (Unisense A/S). The
177 microsensors were connected to a multimeter with pA channels for the H_2 and CO_2 microsensors
178 and a mV channel for the pH microsensor (Unisense A/S). The multimeter was connected to a
179 computer collecting the digitized data. The vertical positions of the microsensor tips were controlled
180 by a motorized micromanipulator connected to the computer, and concentration measurements were
181 done every 50 or 100 μm. Data acquisition was performed with the software Sensor Trace Pro
182 (Unisense A/S). During microsensor profiling the silicone membrane mini-reactor or serum bottle
183 was submerged in a water bath kept at 38 °C. Calibration of the H_2 microsensor was performed in
184 demineralized water by adding various volumes of water saturated with H_2. The H_2 saturated water
185 was slowly extracted with a 10 mL syringe equipped with a 1.2 mm needle, followed by extraction
186 of demineralized water to mix the solution in the syringe in ratios of 25%, 50% and 80% H_2. A new
187 solution was prepared for each concentration. The microsensor was placed in a 15 mL Falcon tube
188 with a stopper where the H_2 solutions were carefully added and the calibration was performed. The
189 solubility of H_2 in water at 38 °C is 728 μmol · L^{-1} at 1 atm pressure according to Crozier and
190 Yamamoto (1974). The calibration of the CO_2 microsensor was done by adding various volumes of
191 a 100 mmol · L^{-1} $KHCO_3$ solution to 0.5 L of acidic water (pH ~1). The pH microsensor was
192 calibrated in standard buffers (VWR chemicals). All calibrations were performed at 38 °C. In the
193 mini-reactor microprofiles of H_2, CO_2 and pH were recorded, while in the methanogenic biofilm
194 only H_2 and pH profiles were recorded.
195

196 2.4 Modelling

197 Modelling of the H_2 reaction rate was performed using the program "Profile" by Berg et al. (1998).
198 A H_2 diffusion coefficient in water at 38 °C of $7.0 \cdot 10^{-5}$ $cm^2 \cdot s^{-1}$ was used (Unisense A/S). The
199 digestate diffusivity (D_s) was described according to $D_s = \varphi \cdot D$ where D is the diffusivity in water
200 and φ is the porosity. The porosity of the digestate with glass beads was 0.63 (Garcia-Robledo et al.
201 2016). In the biofilm, a φ of 0.9 was assumed as this value and thereby (by $D_s = \varphi \cdot D$) derived D_s
202 values previously gave good fits to experimentally derived $\varphi \cdot D_s$ values in a dense biofilm (Glud et
203 al. 1995). The H_2 flux was determined from the H_2 gradient at the surface of the biofilm using
204 Fick's first law of diffusion (Crank 1975) using the same expression for diffusion coefficient as in
205 the modeling approach.

206

207 2.5 Statistics

208 Analysis of variance (ANOVA) and t-tests were performed in R (R version 3.3.1) with the interface
209 R commander (Rcmdr Version 2.2-5).

210

211 2.6 DNA extraction and amplicon sequencing

212 All reactors were sampled for sequencing at the end of the experiments. In replicates containing
213 slurry as well as carrier material both were sampled. DNA was extracted using the FastDNA Spin
214 Kit for Soil (MP Biomedicals, USA) according to the supplier's recommendation. Prior to DNA
215 extraction the slurry or carrier material were subjected to enzyme digestion according to Juretschko
216 et al. (1998). The V4 hypervariable region of the 16S rRNA gene was universally amplified in
217 accordance with previously described protocols (Albertsen et al. 2015), and subsequently barcoded

for sequencing using the Nextera XT protocol (Illumina, USA). The obtained libraries were sequenced in equimolar concentrations on a MiSeq platform using reagent kit v3 (2x300 PE) (Illumina, USA).

The raw sequencing reads were quality checked using trimmomatic (version 0.32) (Bolger et al. 2014) and merged using FLASH (version 1.2.7) (Magoc et al. 2011). The reads were then formatted for use with the UPARSE pipeline (Edgar et al. 2013), screened for chimeric sequences and clustered into Operational Taxonomic Units (OTUs) at 97 % sequence similarity using USEARCH7. Taxonomy was assigned using the RDP algorithm implemented in QIIME (Caporaso et al. 2010) using SILVA database release S132 (Quast et al. 2013). The microbial community data was analyzed using R (version 3.5.2) (R Core Team, 2019) and RStudio (version 1.1.463) (http://www.rstudio.com) using the package ampvis2 (version 2.4.2) (Andersen et al. 2018). Microbial community structure was visualized using heatmaps.

3. Results and discussion

3.1 Time course and dynamics of CO_2 depletion

It has not previously been possible to measure CO_2 microprofiles in chemically aggressive substrates like digester content, and the data presented here are thus the first direct measurements illustrating the spatial effects of CO_2 limitation on hydrogenotrophic methanogenesis. It was possible to investigate this effect by supplying hydrogen to digester content in the previously described membrane mini-reactor. Hydrogen was readily consumed in a narrow zone next to the membrane until the process became CO_2 limited after several hours of flushing with H_2/N_2. Initially, when high CO_2 was still present, H_2 was consumed in a very narrow zone of 0.6 mm next

241 to the membrane at an integrated rate of 0.58 nmol · cm^{-2} · s^{-1}. CO_2 depletion for 10 h led to a pH
242 increase from 8.5 to 9.5. The integrated H_2 consumption rate decreased to 0.22 nmol · cm^{-2} · $s^{-1}$and
243 the H_2 penetration into the slurry increased to 1.7 mm. The surface of the digester content moved
244 1.5 mm during the 10 h due to evaporation (Fig. 1). It should be noted that the CO_2 profiles are
245 dissimilar from normal gas profiles where there is a straight curve through inactive layers between
246 source and sinks. In the CO_2 profiles presented here there is an abrupt decrease at the slurry surface.
247 This is caused by the high bicarbonate concentration in the slurry with which CO_2 is an equilibrium
248 delayed by the slow dehydration of carbonic acid (e.g. Mustaffa et al. 2017). The depletion of CO_2
249 thus led to pH increase, a decrease in H_2 consumption rate and an expansion of the H_2 consumption
250 zone which is consistent with the findings of other studies (Luo et al. 2012; Bassani et al. 2015;
251 Garcia-Robledo et al. 2016). The effect of H_2 addition through silicone membranes/tubing on CO_2
252 and pH will, however, be very local in a full-scale reactor setup where the tubing is submerged in
253 digester content. A localized effect could explain the limited VFA accumulation observed in some
254 studies (Luo and Angelidaki 2013a; Wang et al. 2013). If the effect is local, the potential negative
255 effects of VFA accumulation would not affect the entire reactor until low CO_2 concentrations are
256 present throughout the reactor.

257 A supply of H_2 through silicone membranes or hollow fiber membranes can mediate a full
258 conversion, but the approach is associated with a risk of clogging (Luo and Angelidaki 2013b), and
259 fragility must also be a major problem in a scenario with heterogeneous digester content. The initial
260 maximum specific rate of ~16 nmol H_2 · cm^{-3} · s^{-1} (Fig. 1A) corresponds to a CH_4 production rate of
261 ~8 $L_{CH_4} \cdot L^{-1} \cdot day^{-1}$ which is ~10 times higher than the average CH_4 production rate in the Bånlev
262 biogas reactor. In a biofilm reactor only a minor part of the whole reactor would, however, be
263 occupied with active biofilm, so the actual rate per reactor volume would be much lower.

264 3.2 CO_2 concentration supporting methanogenesis

After CO_2 depletion, CO_2 was stepwise resupplied starting with 2% CO_2 and then gradually increasing the CO_2 concentration to 5, 6, 7, 8, 9, 10, 12, 14, 16, 18, and 20% CO_2. The profiles were allowed to stabilize for 2 h between each increase in CO_2 concentration. It is evident that the H_2 consumption zone moved closer to the membrane and that the H_2 flux increased when the CO_2 concentration was increased (Fig. 2). At 5% CO_2, the H_2 consumption zone was 2.2±0.1 (SD, n=3) mm and the H_2 flux was 0.23±0.01 (SD, n=3) nmol $\cdot$ cm^{-2} $\cdot$ s^{-1}. The addition of 10% CO_2 yielded a consumption zone of 1.3±0.0 (SD, n=3) mm and a H_2 flux of 0.33±0.00 (SD, n=3) nmol $\cdot$ cm^{-2} $\cdot$ s^{-1}. When 18% CO_2 was added the H_2 consumption zone was 1.0±0.1 (SD, n=3) mm and the H_2 flux was 0.45±0.06 (SD, n=3) nmol $\cdot$ cm^{-2} $\cdot$ s^{-1}. Finally, when 20% CO_2 was supplied, the average consumption zone was 1.0±0.1 (SD, n=3) mm and the H_2 flux was 0.52±0.12 (SD, n=3) nmol $\cdot$ cm^{-2} $\cdot$ s^{-1} (Fig. 2). Evaporation resulted in the surface of the digester content moving closer to the silicone membrane during the experiment, decreasing 1.5 mm during the course of the experiment. The surface was always >1 mm away from the H_2 consumption zone (Fig. 2AB), but the loss of water by evaporation might have elevated the microbial density and thereby contributed to the elevated activity. The rise in ion strength might, on the other hand, have decreased the cell-specific activity. A water loss by evaporation could have been avoided by keeping the humidifier vessel at a higher temperature. Analysis of variance (ANOVA) on the data in Fig. 2CD showed a significant effect of CO_2 concentration on both H_2 flux ($p=2.8\cdot10^{-10}$) and width of H_2 consumption zone ($p=3.4\cdot10^{-10}$). The initial H_2 consumption rate of 0.58 nmol $\cdot$ cm^{-2} $\cdot$ s^{-1} obtained from the data in Fig. 1A was not exceeded even when 20% CO_2 was resupplied, resulting in a consumption rate of 0.52 nmol $\cdot$ cm^{-2} $\cdot$ s^{-1}. The initial CO_2 concentration was comparable to a 5% CO_2 supply, but the initial H_2 consumption rate was 60% higher than when 5% CO_2 was re-supplied and the H_2 consumption zone was 3 times wider after the CO_2 re-supply (Figs. 1 and 2). This points to a relatively slow recovery of the H_2 consumption potential after re-introduction of CO_2, and it is likely that some of the

apparently positive effect of CO_2 higher than 5% (Fig. 2) was due to gradual physiological recovery during the period when CO_2 was elevated. Experiments with longer stabilization periods for each stepwise addition of CO_2 did not show any positive effect on H_2 consumption above about 6% CO_2 (Garcia-Robledo et al. 2016), while others have observed inhibition of methanogenesis below 12% CO_2 (Agneessens et al. 2017). Even though the H_2 consumption potential was dependent on the CO_2 availability, it is apparent from Figs. 1 and 2 that CO_2 was always in excess and never fully consumed in the H_2 consumption zone. In environments where methanogens occur, CO_2 concentrations are normally high as in anaerobic digesters (30-50% in the headspace) and it does not appear that there is any microbial selection for high CO_2 affinity. The experiments resulting in Figs. 1 and 2 were repeated 7 times (data not shown), all showing similar chemical profiles and conversion rates.

3.3 Development of a methanogenic biofilm

The CH_4 production rates in the 1 L reactors were determined one, two, five, six, seven and eight weeks after incubation. The CH_4 production rates for both the controls were relatively stable throughout the experiments. The CH_4 production rate for the BIO-BLOK was highest at the beginning of the experiment, decreased during the first 5 weeks of incubation, and then started increasing again after 6 weeks. The CH_4 production rate in the BIO-BLOK was four times higher than the H_2/CO_2 control one and two weeks after incubation, two times higher five and six weeks after incubation, three times higher after seven weeks and four times higher after eight weeks of incubation (Fig. 3). At all time points there was a significant difference (t-test, $p=<0.05$) between the CH_4 production rate of the H_2/CO_2 control and the BIO-BLOK which shows that there is an effect of the presence of the carrier material on the CH_4 production rate. The composition of the microbial community was analyzed by amplicon sequencing and the 15 most abundant operational taxonomic units (OTUS) indentified (Fig. 4), and it appears that the genus *Methanoculleus* was

highly enriched in the biofilm as compared to the treatments without carrier material. Methanogens were thus enriched in the biofilm as hypothesized (Fig. 4). Due to periodic wetting with slurry we still expect significant occurrence of slurry organisms in the biofilm, but syntrophic bacteria like "Syntrophomonadaceae" were present in lower numbers in the biofilm as compared to the N_2/CO_2 control, as were fermentative bacteria like "Clostridia" and "Rikenellaceae".

The CH_4 production rate of the BIO-BLOK decreased until week five where the loading of media and contact with the slurry was increased. The loading of medium and increased contact of the carrier material with the slurry resulted in an increase in the CH_4 production rate, indicating that supply of constituents in the slurry or removal of constituents in the biofilm were essential for optimal biofilm functioning. VFA accumulation was limited and acidification does not seem likely as an explanation for the decrease in the CH_4 production rate. It appears that a biofilm was established within the first week of incubation, and during the following weeks the CH_4 production potential was highly dependent on frequent contact with the slurry. Other studies report stabilization of the biofilm development after 10-90 days (Pérez et al. 1997; Cresson et al. 2008; Brileya et al. 2014; Rachbauer et al. 2016; Pandey and Sarkar 2017) which is reasonably within the timeframe of this study. However, the previous studies on methanogenic biofilms have not attempted to promote biofilm formation by direct exposure to the gas phase. With this approach nutrients were only periodically available, and it appears that nutrient availability may have determined the CH_4 production potential in the present study. Likewise, mineral nutrient addition increased CH_4 production in a fixed-bed biomethanation reactor (Alitalo et al. 2015), suggesting the relevance of nutrient availability during biofilm-based biomethanation. The CH_4 production rate was relatively stable in both the N_2/CO_2 and H_2/CO_2 control throughout the experiment while the biofilm reacted to the change in medium loading and wetting.

3.4 Hydrogen consumption in the biofilm

337 A H_2 microsensor was applied to determine the H_2 concentration profiles in the slurries and
338 biofilms while the bottles were continuously flushed with a mixture of 80% H_2 and 20% CO_2 (Fig.
339 5). Profiles were recorded at several locations in the BIO-BLOK incubations where variation in the
340 H_2 flux and width of the H_2 consumption zone was observed. The consumption zone was up to 0.5
341 mm, the H_2 flux ranged from 0.73-3.11 nmol $\cdot$ $cm^{-2} \cdot s^{-1}$, and the minimum H_2 concentration in the
342 biofilm ranged from 0-400 μmol $\cdot$ L^{-1}. The presence of H_2 in the bottom biofilm layers at some
343 locations illustrate relatively poor biofilm formation at these locations. In the H_2/CO_2 control slurry,
344 the H_2 profiles showed limited variation and the H_2 was fully consumed in a surface zone of 0.9±0.1
345 mm (SD, n=17) mm. Figure 5 shows typical examples of H_2 concentration profiles from slurry and
346 biofilm. The average H_2 flux in the H_2/CO_2 control slurry was 1.14±0.16 (SD, n=17) nmol $\cdot$ $cm^{-2} \cdot s^{-1}$
347 while the H_2 flux at the biofilm/gas interface was 2.11±0.60 (SD, n=40) nmol $\cdot$ $cm^{-2} \cdot s^{-1}$. Hence,
348 the H_2 flux in the BIO-BLOK biofilm was approximately twice as high as the H_2 flux in the H_2/CO_2
349 control slurry and significantly different (t-test, $p=2.5 \cdot 10^{-8}$). This is in agreement with our
350 hypothesis that the carrier material's direct exposure to the gas phase would stimulate biofilm
351 formation and make it more beneficial for the microorganisms to occupy the carrier material than to
352 grow in the slurry. The high rate of H_2 consumption in the biofilm is in accordance with the
353 enrichment of *Methanoculleus* (Fig. 4).

354 3.5 Hydrogen consuming pathway

355 The VFA content in the slurry was analyzed one, five and eight weeks after incubation where
356 acetate was the only detected VFA. In the bottles, acetate concentrations changed at an average rate
357 of -1.63±1.05 (SD, n=3) μmol $\cdot$ d^{-1} in the N_2/CO_2 control, -4.16±2.38 (SD, n=4) μmol $\cdot$ d^{-1} in the
358 H_2/CO_2 control and 6.76±2.20 (SD, n=4) μmol $\cdot$ d^{-1} in the BIO-BLOK slurry between day 10 and
359 38. Between day 38 and 59, the acetate concentrations changed at an average rate of -8.28±1.78
360 (SD, n=4) μmol $\cdot$ d^{-1} in the N_2/CO_2 control, 0.54±0.88 (SD, n=4) μmol $\cdot$ d^{-1} in the H_2/CO_2 control

and 13.64±16.44 (SD, n=4) μmol · d^{-1} in the BIO-BLOK slurry. Acetate was the only VFA that was detected which contradicts inhibition of VFA degradation by H_2 which has been observed in other studies (Luo et al. 2012; Luo and Angelidaki 2013a). In the first part of the experiment, acetate was primarily degraded in both the N_2/CO_2 and H_2/CO_2 control while it accumulated in the BIO-BLOK slurry. In the second part of the experiment, acetate was degraded in the N_2/CO_2 control but accumulated in the H_2/CO_2 control and the BIO-BLOK slurry. The acetate accumulation rate was 25 times higher in the BIO-BLOK compared to the H_2/CO_2 control. The acetate concentration in the present study was ~2-12 times lower in the control and ~3-28 times lower than in H_2 amended reactors reported in other studies (Luo et al. 2012; Agneessens et al. 2017; Agneessens et al. 2018). Acetate mainly accumulates in the start-up phase, but in this study the acetate concentration was measured 1, 5 and 8 weeks after start of incubation which might explain the relatively low acetate concentrations (Mulat et al. 2017; Agneessens et al. 2018). According to our measurements, the CH_4 production accounted for 74-85% of the H_2 consumption in the H_2/CO_2 control. However, the acetate accumulation data indicates that only about 0.1% of the H_2 consumption resulted in net acetate accumulation in the H_2/CO_2 control. The 15-25% discrepancy in the hydrogen addition budget may partially be due to reduction of CO_2 to biomass.

The H_2 flux measurements show a higher flux into the biofilm than into an equivalent area of the surface in the liquid control, reflecting the pronounced enrichment of the genus *Methanoculleus* that is associated mainly with hydrogenotrophic methanogenesis (Dianou et al. 2001; Holmes and Smith 2016) (Fig. 4). The comparatively higher H_2 influx into the biofilm means that the CH_4 production in the BIO-BLOK reactors should have been even higher as compared to the H_2/CO_2 controls than the difference in surface area indicates. The CH_4 production rate in the BIO-BLOK incubations was, however, only 2-4 times higher than in the H_2/CO_2 control, in spite of the carrier material surface area being 7-8 times higher, indicating that the entire surface area might not have been

385 colonized. The high H_2 flux as compared to the total CH_4 production rate could also have been due
386 to high rates of homoacetogenesis. However, only 0-0.2% of the H_2 consumption resulted in net
387 acetate accumulation in the BIO-BLOK slurry. The pH at the surface of the biofilm was determined
388 in two locations of the biofilm with a pH microelectrode at day 58, and the pH was 7.6 and 8.1
389 which is in agreement with very limited acetate accumulation. Hence, homoacetogenesis does not
390 explain the discrepancy between the H_2 flux and CH_4 production rate, and limited colonization of
391 the carrier material appears as the most likely explanation. A contributing factor to the apparent
392 discrepancy could be that the surface area stated by the BIO-BLOK supplier might not be realized
393 when a relatively thick biofilm is covering the material.
394 The N_2/CO_2 control produced CH_4 throughout the experiment, confirming breakdown of organic
395 matter to sustain methanogenesis at low rates. The methanogenesis persisted although 40% of the
396 inoculum was exchanged with mineral medium and only a limited amount of complex organic
397 matter must have remained.
398
399 3.6 Fitting carrier material in a full-scale reactor
400 The biogas reactor at Foulum biogas plant (Tjele, Denmark) was used as a point of reference for
401 calculating the amount of carrier material needed in a reactor. The headspace was assumed to be
402 75% of the total reactor volume and the carrier material to occupy 15% of the total volume of the
403 reactor. The calculations are based on the H_2 flux in the BIO-BLOK incubations. The H_2
404 consumption was assumed independent of CO_2 concentration above 20% and linearly decrease to
405 half of the 20% rate when the CO_2 concentration was 2% (according to the data in Fig. 2). The H_2
406 flux was assumed to respond to the H_2 concentration according to $J = \sqrt{\frac{2 \cdot D \cdot C}{R}}$, where J is the H_2
407 flux ($mol \cdot m^{-2} \cdot h^{-1}$), D is the diffusion coefficient ($m^2 \cdot h^{-1}$), C is the H_2 concentration at the biofilm
408 surface ($mol \cdot m^{-3}$) and R is the specific H_2 consumption rate ($mol \cdot m^{-3} \cdot h^{-1}$) (Revsbech et al. 1980).

The surface of the BIO-BLOK was assumed to be the 300 m^2 m^{-3} claimed by the company. The initial CO_2 content of the biogas was assumed to be 50% and H_2 was added in a four times volumetric equivalent. If a CH_4 content of >95% is required (Weiland 2010) a retention time of ~4 days is necessary with such a reactor configuration. Assuming this concentration dependency of the H_2 consumption rate, the H_2 consumption substantially slows down at low concentrations. If the carrier material occupies 75% of the total volume of the reactor, the retention time necessary would decrease to one day. The carrier material should be fitted in the reactor in a fashion that would allow supply of nutrients to the biofilm. This could be achieved by periodically sprinkling the carrier material with digester content. Since digester content is rather heterogeneous and contain fragments of organic matter that are only partially degraded it would be necessary to sieve/filtrate the digester content (as was done in this study) to allow for sprinkling. This would also aid in preventing clogging of the biofilm carrier material with non-biofilm material. The biofilm would remain moist by the sprinkling, water vapor in the biogas and the H_2O produced during hydrogenotrophic methanogenesis. Apart from the benefit of a very efficient mass transfer, the problems with pH increase would be minimal since methanogenesis relies on the CO_2 in the gas phase and not the bicarbonate pool in the digester content. Any metabolic effect on pH in the biofilm will thus not be due to the catabolic metabolism, but there could be minor effects by anabolic metabolism. The biofilm approach tested in this investigation is in principle similar to the trickling filter approach tested by Rachbauer et al. (2016), but the mass transfer was by our approach facilitated by not having the hydrogen influx into the biofilm slowed down by diffusion through a water layer above the biofilm. A similar effect could have been obtained by only periodic watering of the trickling filter biofilm.

4. Conclusion

The successful application of H_2 addition to bioreactors is highly dependent on efficient gas-to-liquid mass transfer and on controlling the negative effects of CO_2 limitation leading to pH increase. The microbial community partially recovers after CO_2 depletion, but hydrogenotrophic methanogenesis is highly dependent on CO_2 concentration and there appears to been no selection for low CO_2 affinity. Carrier material allowed for establishing a methanogenic biofilm for biogas upgrading that was dominated by the genus *Methanoculleus* that is known to be associated with hydrogenotrophic methanogenesis. A bioreactor based on a gas-exposed methanogenic biofilm could lower the gas-to-liquid mass transfer limitations as well as the negative effects of CO_2 depletion and pH increase.

Conflict of interest

The authors declare that they have no conflict of interest.

Acknowledgement

This study was supported by the Innovation Fund Denmark project Electrogas, grant no. 4106-00017B, and by the Poul Due Jensen Foundation. We are grateful for the technical support of Lars Borregaard Petersen and Preben Sørensen.

451 References

452

453 1. Agneessens, L. M., Ottosen, L. D. M., Voigt, N. V., Nielsen, J. L., de Jonge, N., Fischer, C. H.,
454 Kofoed. M. V. W., 2017. In-situ biogas upgrading with pulse H_2 additions: The relevance of
455 methanogen adaption and inorganic carbon level. Bioresour. Technol. 233, 256–263.

456

457 2. Agneessens, L. M., Ottosen, L. D. M., Andersen, M., Olesen, C. B., Feilberg, A., Kofoed, M. V.
458 W., 2018. Parameters affecting acetate concentrations during in-situ biological hydrogen
459 methanation. Bioresour. Technol. 258, 33–40.

460

461 3. Albertsen, M., Karst, S.M., Ziegler, A.S., Kirkegaard, R.H., Nielsen, P.H., 2015. Back to Basics
462 – The Influence of DNA Extraction and Primer Choice on Phylogenetic Analysis of Activated
463 Sludge Communities. PLoS One 10, e0132783.

464

465 4. Alitalo, A., Niskanen, E., Aura, E., 2015. Biocatalytic methanation of hydrogen and carbon
466 dioxide in a fixed bed bioreactor. Bioresour. Technol. 196, 600-605.

467

468 5. Alvarez-Galvan, M. C., Mota, N., Ojeda, M., Rojas, S., Navarro, R. M., Fierro, J. L. G., 2011.
469 Direct methane conversion routes to chemicals and fuels. Catal. Today 17, 15–23.

470

471 6. Andersen, K. S., Kirkegaard, R. H., Karst, S. M., Albertsen, M., 2018. ampvis2: an R package to
472 analyse and visualise 16S rRNA amplicon data. *bioRxiv*.

473

7. Angelidaki, I., Alves, M., Bolzonella, D., Borzacconi, L., Campos, J. L., Guwy, A. J., Kalyuzhnyi, S., Jenicek, P., van Lier, J. B., 2009. Defining the biomethane potential (BMP) of solid organic wastes and energy crops: a proposed protocol for batch assays. Wat. Sci. Tech. 59.5, 927-934.

8. Angelidaki, I., Karakashev, D., Batstone, D. J., Plugge, C. M., Stams, A. J. M., 2011. Biomethanation and Its Potential. Methods Enzymol. 494, 327-351.

9. Angelidaki, I., Treu, L., Tsapekos, P., Luo, G., Campanaro, S., Wenzel, H., Kougias, P. G., 2018. Biogas upgrading and utilization: Current status and perspectives. Biotechnol. Adv. 36, 452-466.

10. Bassani, I., Kougias, P. G., Treu, L., Angelidaki, I., 2015. Biogas Upgrading via Hydrogenotrophic Methanogenesis in Two-Stage Continuous Stirred Tank Reactors at Mesophilic and Thermophilic Conditions. Environ. Sci. Technol. 49, 12585−12593.

11. Bassani, I., Kougias, P. G., Angelidaki, I., 2016. In-situ biogas upgrading in thermophilic granular UASB reactor: key factors affecting the hydrogen mass transfer rate. Bioresour. Technol. 221, 485–491.

12. Berg, P., Risgaard-Petersen, N., Rysgaard, S., 1998. Interpretation of measured concentration profiles in sediment pore water. Limnol. Oceanogr. 43, 1500-1510.

13. Bolger, A.M., Lohse, M., Usadel, B., 2014. Trimmomatic: a flexible trimmer for Illumina sequence data. Bioinformatics 30, 2114–2120.

14. Brileya, K. A., Camilleri, L. B., Zane, G. M., Wall, J. D., Fields, M. W., 2014. Biofilm growth mode promotes maximum carrying capacity and community stability during product inhibition syntrophy. Front. Microbiol. 5, 693.

15. Caporaso, J.G., Kuczynski, J., Stombaugh, J., Bittinger, K., Bushman, F.D., Costello, E.K., Fierer, N., Peña, A.G., Goodrich, J.K., Gordon, J.I., Huttley, G.A., Kelley, S.T., Knights, D., Koenig, J.E., Ley, R.E., Lozupone, C.A., McDonald, D., Muegge, B.D., Pirrung, M., Reeder, J., Sevinsky, J.R., Turnbaugh, P.J., Walters, W.A., Widmann, J., Yatsunenko, T., Zaneveld, J., Knight, R., 2010. QIIME allows analysis of high-throughput community sequencing data. Nat. Methods 7, 335–336.

16. Cord-Ruwisch, R., Mercz, T. I., Hoh, C., Strong, G. E., 1997. Dissolved Hydrogen Concentration as an On-Line Control Parameter for the Automated Operation and Optimization of Anaerobic Digesters. Biotechnol. Bioeng. 56, 626-634.

17. Crank, J., 1975. The Mathematics of Diffusion, second ed. Oxford University Press. Oxford.

18. Cresson, R., Escudié, R., Steyer, J-P., Delgenés, J-P., Bernet, N., 2008. Competition between planktonic and fixed microorganisms during the start-up of methanogenic biofilm reactors. Water Res. 42, 792-800.

19. Crozier, T. E., and Yamamoto, S., 1974. Solubility of hydrogen in water, sea water, and sodium chloride solutions. J. Chem. Eng. Data 19, 242–244.

20. Demirel, B., Scherer, P., 2008. The roles of acetotrophic and hydrogenotrophic methanogens

521 during anaerobic conversion of biomass to methane: a review. Rev. Environ. Sci. Biotechnol. 7,
522 173–190.

523 21. Díaz, I., Pérez, C., Alfaro, N. and Fdz-Polanco, F., 2015. A feasibility study on the
524 bioconversion of CO_2 and H_2 to biomethane by gas sparging through polymeric membranes.
525 Bioresour. Technol. 185, 246–253.

526 22. Dianou, D., Miyaki, T., Asakawa, S., Morii, H., Nagaoka, K., Oyaizu, H., Matsumoto, S., 2001.
527 Methanoculleus chikugoensis sp. nov., a novel methanogenic archaeon isolated from paddy field
528 soil in Japan, and DNA–DNA hybridization among Methanoculleus species. Int. J. Syst. Evol.
529 Microbiol. 51, 1663–1669.

530 23. Edgar, R.C., 2013. UPARSE: highly accurate OTU sequences from microbial amplicon reads.
531 Nat. Methods 10, 996–998.

532 24. Gagliano, M. C., Ismail, S. B, Stams, A. J. M., Plugge, C. M., Temmink, H., Van Lier, J. B.,
533 2017. Biofilm formation and granule properties in anaerobic digestion at high salinity. Water Res.
534 12, 61-71.
535
536 25. Gaj, K., 2017. Applicability of selected methods and sorbents to simultaneous
537 removal of siloxanes and other impurities from biogas. Clean Techn. Environ. Policy 19, 2181–
538 2189.
539
540 26. Garcia-Robledo, E., Ottosen, L. D. M., Voigt, N. V., Kofoed, M. V., Revsbech, N. P., 2016.
541 Micro-scale H_2–CO_2 Dynamics in a Hydrogenotrophic Methanogenic Membrane Reactor. Front.
542 Microbiol. 7, 1276.

543 27. Ghorbanian, M., Lupitskyy, R. M., Satyavolu, J. V. and Berson, R. E., 2014. Impact of
544 Supplemental Hydrogen on Biogas Enhancement and Substrate Removal Efficiency in a Two-Stage
545 Expanded Granular Sludge Bed Reactor. Environ. Eng. Sci. 31, 253-260.

546 28. Götz, M., Lefebvre, J., Mörs, J., Koch, A. M., Graf, F., Bajohr, S., Reimert, R., Kolb, T., 2016.
547 Renewable Power-to-Gas: A technological and economic review. Renew. Energy 85, 1371-1390.
548

549 29. Holmes, D. E., Smith, J. A., 2016. Biologically Produced Methane as a Renewable Energy
550 Source, in: Sariaslani, S., Gadd, G. M. (Eds.), Advances in Applied Microbiology. Academic Press,
551 pp. 1-41.
552

553 30. Jensen, M. B., Kofoed, M. V. W., Fischer, K., Voigt, N. V., Agneessens, L. M., Batstone, D. J.,
554 Ottosen, L. D. M., 2018. Venturi-type injection system as a potential H_2 mass transfer technology
555 for full-scale in situ biomethanation. Appl. Energ. 222, 840–846.
556

557 31. Jeroschewski, P., Steuckart, C. and Kühl, M., 1996. An Amperometric Microsensor for the
558 Determination of H_2S in Aquatic Environments. Anal. Chem. 68, 4351-4357.

559 32. Juretschko, S., Timmermann, G., Schmid, M, Schleifer, K-H., Pommerening-Röser, A., Koops,
560 H-P., Wagner, M., 1998. Combined Molecular and Conventional Analyses of Nitrifying Bacterium
561 Diversity in Activated Sludge: Nitrosococcus mobilis and Nitrospira-Like Bacteria as Dominant
562 Populations. App. Environ. Microbiol. 64, 3042–3051.

563 33. Liu, R., Hao, X. Wei, J., 2016. Function of homoacetogenesis on the heterotrophic methane
564 production with exogenous H_2/CO_2 involved. Chem. Eng. J. 284, 1196–1203.
565

566 34. Luo, G., Johansson, S., Boe, K., Xie, L., Zhou, Q. and Angelidaki, I., 2012. Simultaneous
567 Hydrogen Utilization and In Situ Biogas Upgrading in an Anaerobic Reactor. Biotechnol. Bioeng.
568 109, 1088-1094.

569 35. Luo, G., Angelidaki, I., 2013a. Hollow fiber membrane based H_2 diffusion for efficient in situ
570 biogas upgrading in an anaerobic reactor. Appl. Microbiol. Biotechnol. 97, 3739–3744.

571 36. Luo, G., Angelidaki, I., 2013b. Co-digestion of manure and whey for in situ biogas upgrading
572 by the addition of H_2: process performance and microbial insights. Appl. Microbiol. Biotechnol. 97,
573 1373–1381.

574 37. Magoč, T., Salzberg, S.L., 2011. FLASH: fast length adjustment of short reads to improve
575 genome assemblies. Bioinformatics 27, 2957–2963.

576 38. Mulat, D. G., Mosbæk, F., Ward, A. J., Polag, D., Greule, M., Keppler, F., Nielsen, J. L.,
577 Feilberg, A., 2017. Exogenous addition of H_2 for an in situ biogas upgrading through biological
578 reduction of carbon dioxide into methane. Waste Manage. 68, 146-156.
579

580 39. Mustaffa, N. I. H., Stribel, M., Wurl, O. 2017. Enrichment of Extracellular Carbonic Anhydrase
581 in the Sea Surface Microlayer and Its Effect on Air-Sea CO_2 Exchange. Geophys. Res. Lett. 44,
582 12324-12330.
583

584 40. Nielsen, M., Larsen, L. H., Ottosen, L. D. M., Revsbech, N. P., 2015. Hydrogen microsensors
585 with hydrogen sulfide traps. Sens. Actuators, B 215, 1–8.
586

587 41. Quast, C., Pruesse, E., Yilmaz, P., Gerken, J., Schweer, T., Yarza, P., Peplies, J., Glöckner, F.
588 O., 2013. The SILVA ribosomal RNA gene database project: improved data processing and web-
589 based tools. Nucleic Acids Res. 41, 590–596.
590
591 42. Rachbauer, L. Voitl, G., Bochmann, G., Fuchs, W., 2016. Biological biogas upgrading capacity
592 of a hydrogenotrophic community in a trickle-bed reactor. Appl. Energ. 180, 483–490.
593
594 43. Revsbech, N. P., Jørgensen, B. B., Blackburn, T. H., 1980. Oxygen in the Sea Bottom Measured
595 with a Microelectrode. Science 207, 1355-1356.
596
597 44. R Core Team (2019). R: A language and environment for statistical computing. R Foundation
598 for Statistical Computing, Vienna, Austria. http://www.R-project.org/.
599
600 45. Revsbech, N.P., Garcia-Robledo, E., Sveegaard, S., Andersen, M. H., Gothelf, K. V., Larsen, L.
601 H., 2019. Amperometic microsensor for measurement of gaseous and dissolved CO_2. Sens.
602 Actuators, B, 283, 349-354.
603
604 46. Schmidt, J. E., Ahring, B., 1993. Effects of Hydrogen and Formate on the Degradation of
605 Propionate and Butyrate in Thermophilic Granules from an Upflow Anaerobic Sludge Blanket
606 Reactor. Appl. Environ. Microbiol. 59, 2546-2551.
607
608 47. Pandey, S. and Sarkar, S., 2017. Anaerobic treatment of wastewater using a two-stage packed-
609 bed reactor containing polyvinyl alcohol gel beads as biofilm carrier. J. Environ. Chem. Eng. 5,
610 1575–1585.

48. Pérez, M., Romero, L. I., Nebot, E., Sales, D., 1997. Colonisation of porous sintered-glass support in anaerobic thermophilic bioreactors. Bioresour. Technol. 59, 177-183.

49. Wang, W., Xie, L., Luo, G., Zhou, Q., Angelidaki, I., 2013. Performance and microbial community analysis of the anaerobic reactor with coke oven gas biomethanation and in situ biogas upgrading. Bioresour. Technol. 146, 234–239.

50. Weiland, P., 2010. Biogas production: current state and perspectives. Appl. Microbiol. Biotechnol. 85, 849–860.

621 Figure captions

622 Figure 1: Profiles in membrane reactor 1 h after addition of slurry while supplied with 75% H_2 and
623 25% N_2 below the membrane (A+C). Profiles in the reactor 10 h after supplying with a gas mixture
624 of 75% H_2 and 25% N_2 (B+D). H_2 (○), CO_2 (●), pH (●), modelled H_2 concentration (black line) and
625 modelled H_2 consumption rate (red line box). The depth scale is the reading on the
626 micromanipulator. The surface of the silicone membrane was at 6 mm on that scale. The surface of
627 the slurry decreased from 0.8 to 2.6 mm during the 10 h of CO_2 depletion.

628 Figure 2: Selected H_2 (A) and CO_2 (B) concentration profiles when a mixture of 75% H_2 and 5%
629 (●), 10% (○), 18% (◆) or 20% (◇) CO_2 was supplied. Note different scale on horizontal axis. The
630 depth scale is the reading on the micromanipulator. The surface of the silicone membrane was at 6
631 mm on that scale. The surface of the slurry decreased from 2.7 to 3.4 mm during the experiment.
632 The H_2 flux and width of consumption zone as a function of CO_2 supply are plotted in panels C and
633 D, respectively.

634 Figure 3: Average CH_4 production rate (± SD, n=4) as a function of time for the N_2/CO_2 control
635 (filled circle), H_2/CO_2 control (filled square) and BIO-BLOK (filled diamond).

636 Figure 4: Examples of H_2 concentration profiles. H_2 concentration profiles in the control H_2/CO_2
637 slurry (left) and BIO-BLOK biofilm (right).

638 Figure 5: Microbial community analysis. Heat map of read abundance showing the 15 most
639 abundant OTUs.

640

641

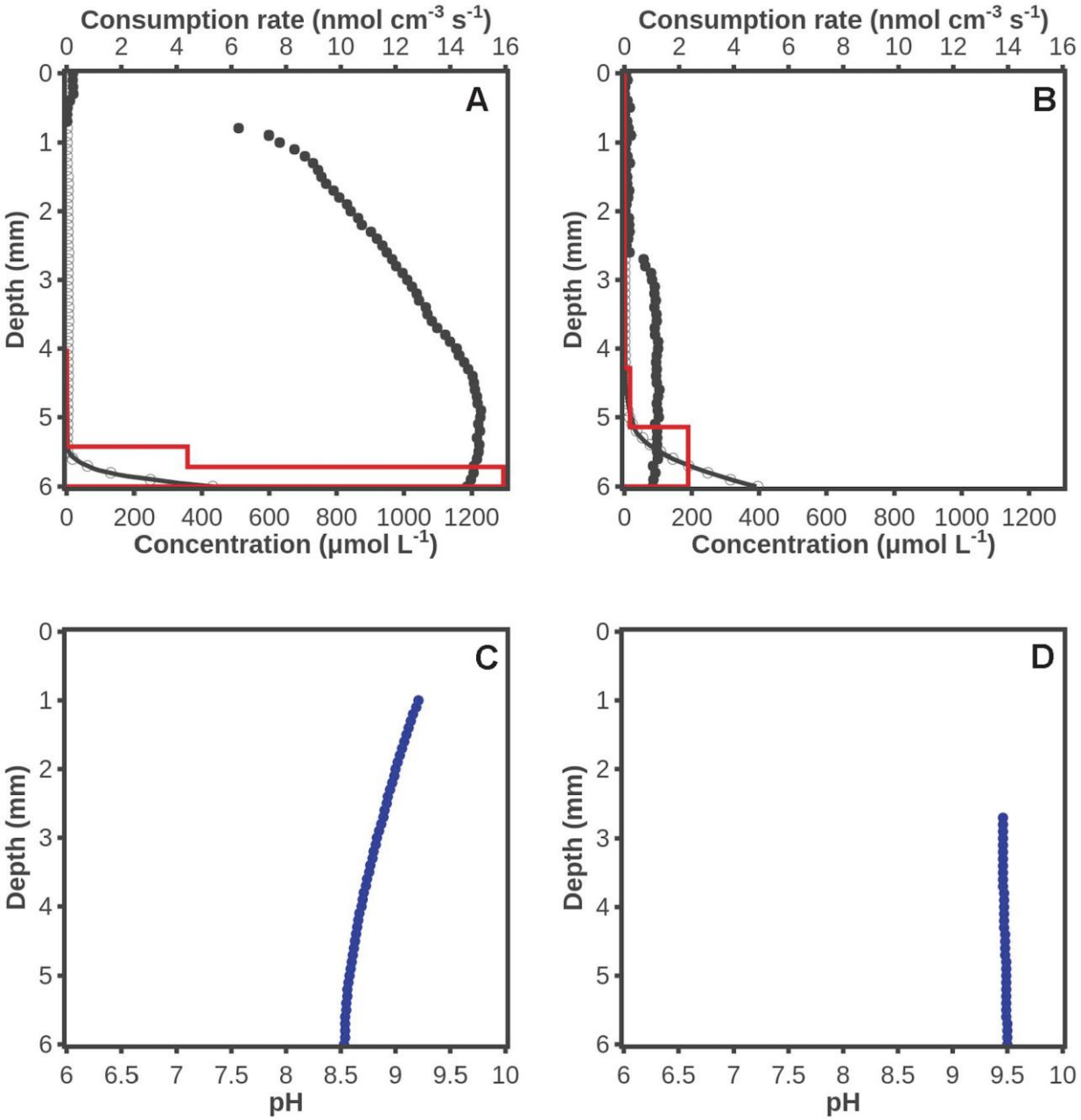
Consumption rate (nmol cm-3 s-1)
A
B
Depth (mm)
Concentration (µmol L-1)
C
D
pH

642

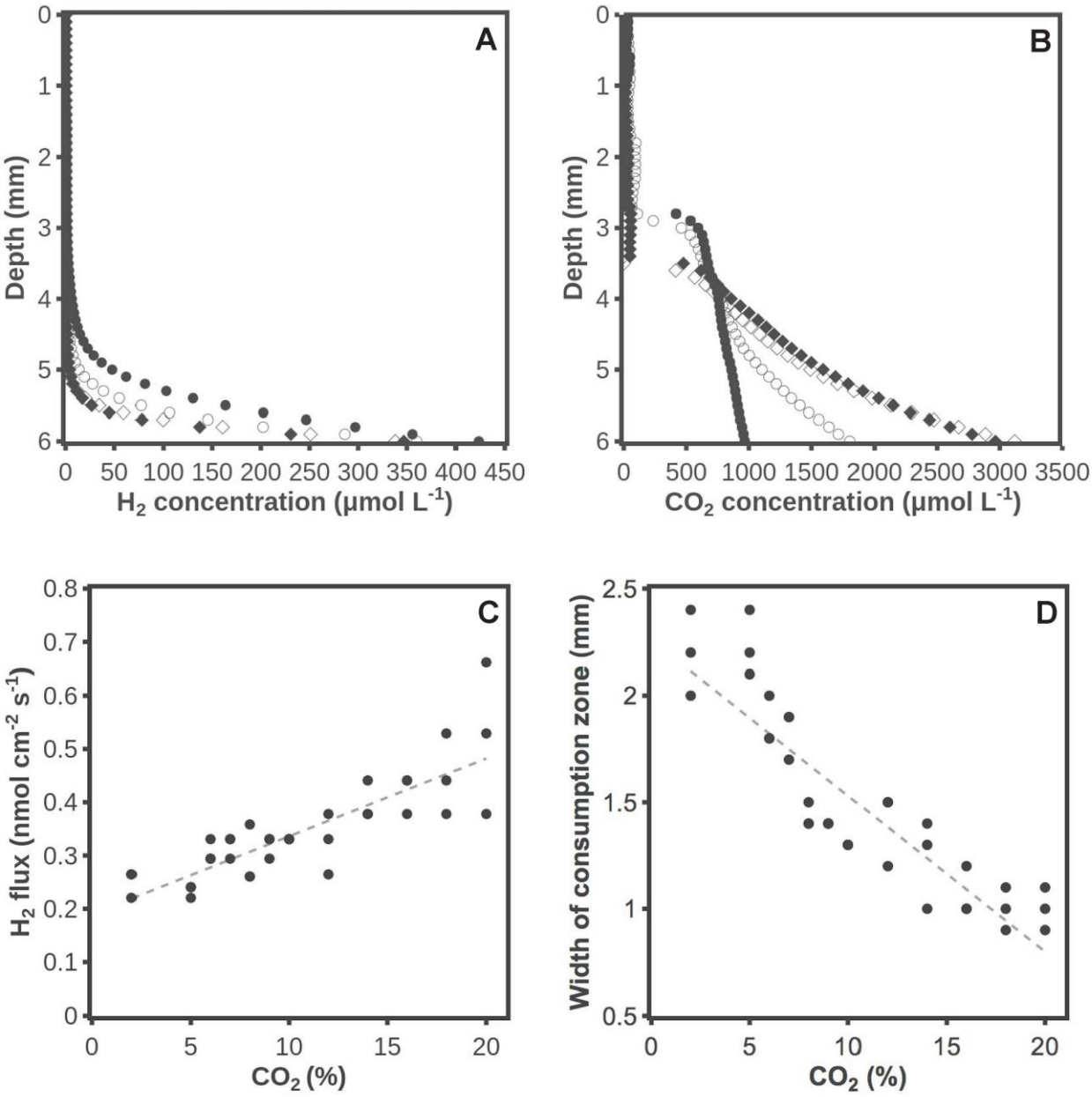

643

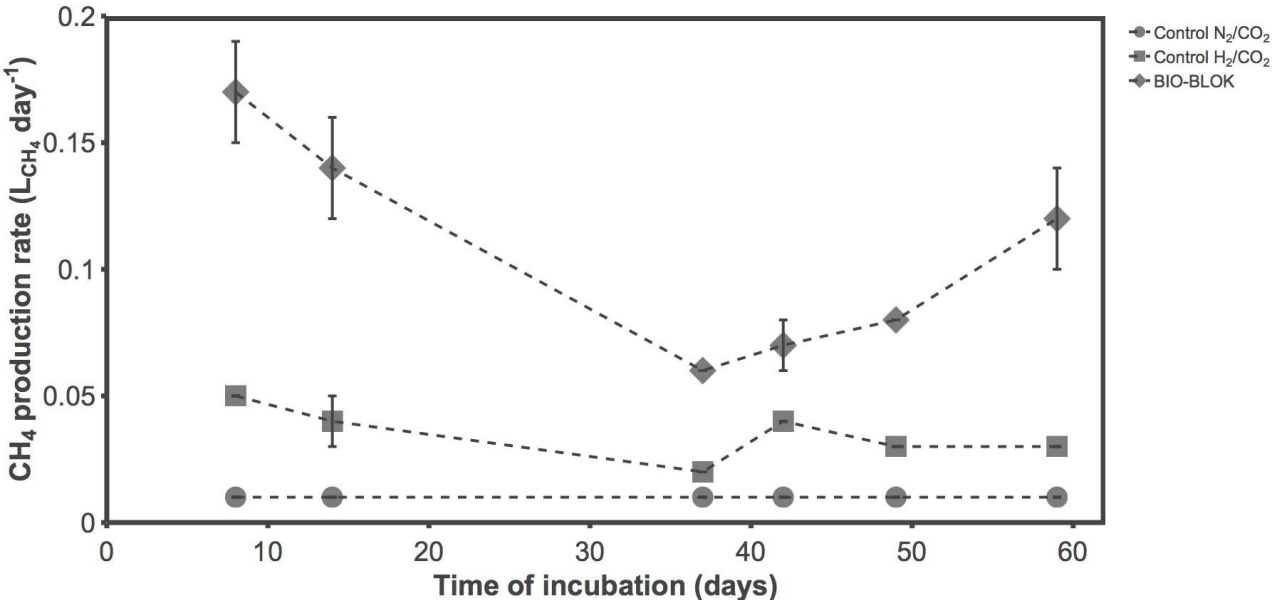
Control N_2/CO_2
Control H_2/CO_2
BIO-BLOK
CH_4 production rate (L_{CH_4} day^{-1})
0.2
0.15
0.1
0.05
0
0
10
20
30
40
50
60
Time of incubation (days)

644


Control N_2/CO_2
Control H_2/CO_2
BIO-BLOK slurry
BIO-BLOK carrier
Methanoculleus 9.8 10.3 9 10 10.4 9.1 8.4 10.3 4.2 6.1 8.5 7.4 24.3 28.6 24.8 23.3
Syntrophomonadaceae 9.3 8.5 9.5 9.7 6.4 8.3 10.6 7.1 8.2 7.3 6.2 7.1 4.5 5.1 4.2 4.5
Clostridia 8.5 10.6 9.1 8.2 7.4 6.2 4.8 5.9 6.3 5.9 6.3 4.9 4.3 3.3 4.1 3.8
Rikenellaceae 6.3 7.5 7.4 6.3 6.5 6.7 4.5 6.4 5 6.9 7.3 6.8 3.8 3.7 4.8 3.8
W27 2 2.1 2.2 2.6 8.7 6.9 6.2 8.4 6.7 7.7 8 5.9 5.2 3 4.3 3.3
DMER64 5.3 6.3 6.3 5.5 5.4 5.7 3.9 5.2 4.3 5.7 5.7 5.7 2.9 3 4 3.2
Fastidiosipila 3 3.1 4.2 3.3 2.8 2.4 2.6 2.5 3 2.7 2.9 2.2 3.1 6.7 5.7 5.1
MBA03 2.1 1.5 1.4 1.8 2.5 3 2.9 3.1 4.1 3.7 3.4 4.4 4.3 3.5 3 4.6
MBA03 2.2 1.7 1.5 1.9 2.6 3.1 2.6 3 4.1 3.8 3.5 4 3.6 3.3 2.9 4.1
Ruminococcaceae 5 4.8 4.8 4.5 3.3 2.9 3.6 3 2.6 2.6 2.5 2.2 1.6 1.3 1.6 1.2
Lentimicrobiaceae 4.9 4.8 4.7 4.7 1.1 2.3 1 1.3 3.1 1.6 2.7 2.5 1.5 1.1 1.7 2.2
MBA03 1.6 1.3 1.1 1.4 1.8 2 1.9 2 2.8 2.4 2.3 2.7 2.4 2.2 2.1 3
ST-12K33 3.3 3.8 3.8 3 2.1 1.8 1.4 1.8 1.5 1.8 2.1 1.6 0.8 0.7 1 0.8
Alkaliphilus 1.2 0.5 0.5 1.3 1.7 2 2.5 1.9 2.5 2.3 1.6 3.5 2.3 1.7 1.8 2.3
MBA03 1.2 0.9 0.8 1.2 1.6 1.7 1.9 1.6 2.4 2.1 2.1 2.3 2.7 2 1.7 2.7
% Read Abundance
10.0
1.0
0.1

645

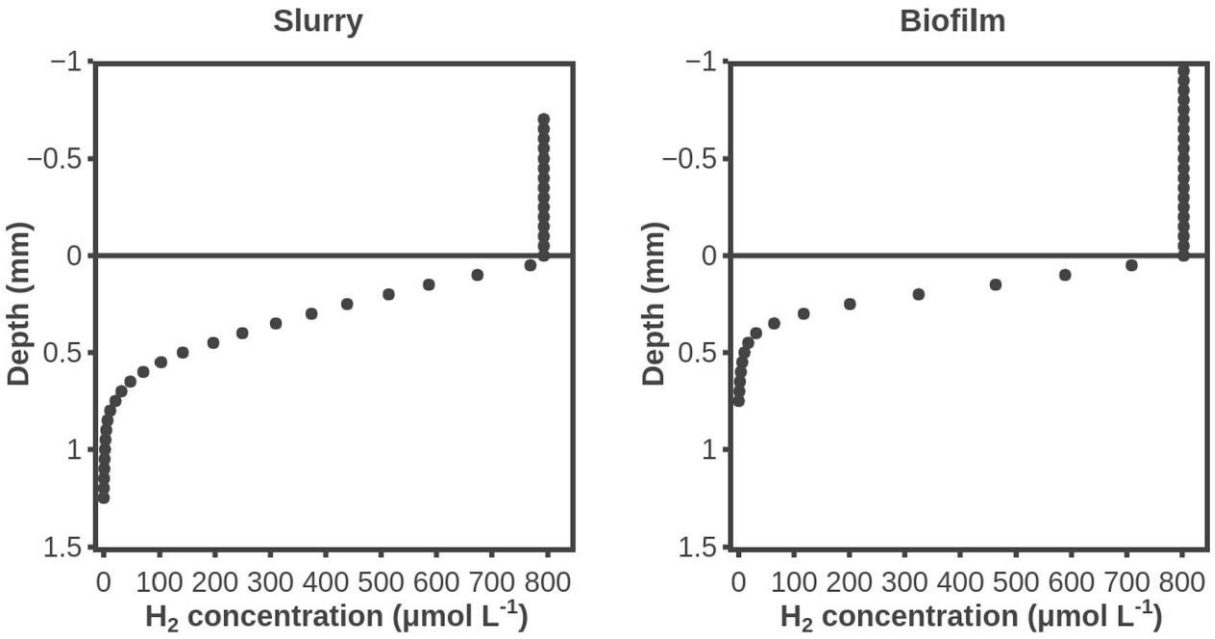

646

647

Highlights

- Hydrogen addition resulted in CO_2 limitation and pH increase
- Hydrogenotrophic methanogenesis was highly dependent on CO_2 concentration
- A methanogenic biofilm was established on carrier material
- The methanogenic biofilm had a high rate of methanogenesis
- The methanogenic biofilm was enriched in the genus *Methanoculleus*